J Membrane Biol (2014) 247:883–895
DOI 10.1007/s00232-014-9690-8

RESEARCH ARTICLES

Molecular Dynamics Simulations of a Membrane Protein/Amphipol Complex

Jason D. Perlmutter · Jean-Luc Popot · Jonathan N. Sachs

Received: 21 January 2014 / Accepted: 22 May 2014 / Published online: 15 June 2014

Abstract Amphipathic polymers known as "amphipols" provide a highly stabilizing environment for handling membrane proteins in aqueous solutions. A8-35, an amphipol with a polyacrylate backbone and hydrophobic grafts, has been extensively characterized and widely employed for structural and functional studies of membrane proteins using biochemical and biophysical approaches. Given the sensitivity of membrane proteins to their environment, it is important to examine what effects amphipols may have on the structure and dynamics of the proteins they complex. Here we present the first molecular dynamics study of an amphipol-stabilized membrane protein, using *Escherichia coli* OmpX as a model. We begin by describing the structure of the complexes formed by supplementing OmpX with increasing amounts of A8-35, in order to determine how the amphipol interacts with the transmembrane and extramembrane surfaces of the protein. We then compare the dynamics of the protein in either A8-35, a detergent, or a lipid bilayer. We find that protein dynamics on all accessible length scales is restrained by A8-35, which provides a basis to understanding some of the stabilizing and functional effects of amphipols that have been experimentally observed.

Keywords OmpX · A8-35 · Surfactants · Dynamics

Abbreviations

2D	Two-dimensional
A8-35	A poly(sodium acrylate)-based amphipol comprising ~35 % of free carboxylates, ~25 % of octyl chains, ~40 % of isopropyl groups
APol	Amphipol
CG	Coarse-grain
DDM	*n*-Dodecyl-β-D-maltopyranoside
DHPC	Dihexanoylphosphatidylcholine
DOPC	Dioleoylphosphatidylcholine
EM	Electron microscopy
FWHM	Full width at half-maximum
MD	Molecular dynamics
MP	Membrane protein
OmpX	Outer membrane protein X from *Escherichia coli*
PCA	Principal component analysis
RCG	Reverse coarse-grain
RMSF	Root mean squared fluctuations
SERCA1a	The fast twitch sarcoplasmic calcium pump

Introduction

Amphipathic polymers known as amphipols (APols) have been developed as stabilizing surfactants for handling membrane proteins (MPs) in aqueous solutions (Popot et al. 2011; Zoonens and Popot 2014). The best characterized APol, called A8-35, consists of a polyacrylate

J. D. Perlmutter (✉)
Department of Physics, Brandeis University, 415 South Street, Waltham, MA 02453, USA
e-mail: perlm@brandeis.edu

J.-L. Popot
Laboratoire de Biologie Physico-Chimique des Protéines Membranaires, UMR 7099, CNRS/Université Paris 7, Institut de Biologie Physico-Chimique (FRC 550), 13 rue Pierre et Marie Curie, 75005 Paris, France

J. N. Sachs
Department of Biomedical Engineering, University of Minnesota, 312 Church Street SE, Minneapolis, MN 55455, USA

backbone with ~25 % octyl grafts, ~40 % isopropyl grafts, and ~35 % ungrafted carboxylates (Tribet et al. 1996). In aqueous solutions, A8-35 spontaneously assembles, above a critical concentration of ~0.002 g L^{-1} (Giusti et al. 2012), into small, well-defined, globular particles resembling detergent micelles, which have been extensively characterized by a variety of biophysical techniques (Gohon et al. 2004; 2006; Tehei et al. 2014) and modeled by coarse-grain (CG) and all-atom molecular dynamics (MD) (Perlmutter et al. 2011). MD data indicate that the particles feature, as expected, a hydrophobic core, rich in octyl chains, and a hydrophilic surface, rich in free carboxylates. They also predict that the surface of A8-35 particles is more viscous than that of detergent micelles, and even that of lipid bilayers. This first MD work established that the CG approach, which has been used in the present study, is reliable in the sense that only minor adjustments are observed upon moving back to the full-atom representation during a reverse coarse-graining procedure (Perlmutter et al. 2011).

A8-35 has been used to complex and keep water-soluble a wide range of MPs, most of which are much more stable as MP/APol complexes than they are in detergent solution, which has led to a large variety of structural and functional studies (reviewed in Popot et al. 2011; Zoonens and Popot 2014). Its interactions with MPs have been characterized by radiation scattering, size exclusion chromatography, analytical ultracentrifugation, NMR, cryo-electron microscopy (EM), Förster resonance energy transfer, and various other approaches (see e.g., Zoonens et al. 2005, 2007; Gohon et al. 2008; Catoire et al. 2009, 2010; Popot et al. 2011; Althoff et al. 2011; Liao et al. 2013, 2014; Huynh et al. 2014). These studies provide a consistent picture of MP/APol complexes, according to which the polymer specifically adsorbs onto the transmembrane, hydrophobic surface of the protein (Zoonens et al. 2005; Catoire et al. 2009, 2010; Popot et al. 2011; Althoff et al. 2011; Liao et al. 2013, 2014; Etzkorn et al. 2014, Planchard et al. 2014), forming a layer 1.5–2-nm thick (Gohon et al. 2008; Popot et al. 2011; Althoff et al. 2011). Functionally, the situation is variegated. Most MPs are functional following complexation by APols (reviewed in Popot 2010; Popot et al. 2011; Zoonens and Popot 2014). In some cases (Martinez et al. 2002; Gohon et al. 2008), their behavior as MP/APol complexes resembles that in the membrane more than that in detergent solution, which, at least in the case of bacteriorhodopsin (BR), has been traced to APols allowing the rebinding of lipids that had been displaced by the detergent (Dahmane et al. 2013). The sarcoplasmic calcium pump SERCA1a, however, is both reversibly inhibited and strongly stabilized by APols (Champeil et al. 2000). The existence of an intriguing correlation between the two effects (Picard et al. 2006) has suggested the "Gulliver effect" hypothesis, which posits, in reference to Swift's character being tied down by the Lilliputians (Swift 1726), that multipoint binding of APols to the protein's hydrophobic surface may damp large-scale conformational excursions of the transmembrane domain (Popot et al. 2003, 2011; Picard et al. 2006). This speculation, which seems to tally with the higher viscosity of A8-35 particles as compared to detergent micelles suggested by MD calculations (Perlmutter et al. 2011), has recently received some experimental support: folding/unfolding studies have shown that OmpA, a small β-barrel MP from the outer membrane of *Escherichia coli*, is stabilized by A8-35 kinetically, not thermodynamically, due to the presence of a higher free-energy barrier to unfolding as compared to that in detergent solution (Pocanschi et al. 2013). No direct evidence has been provided to date, however, that trapping by APols actually affects the dynamics of MPs.

We present here the first computational model of a MP/APol complex, developed with the goal of fostering a better understanding of the effects of the polymer on the protein's structure and dynamics. The model protein is OmpX from the outer membrane of *E. coli*, a small 8-strand β-barrel protein whose structure has been established by both X-ray crystallography (Vogt and Schulz 1999), and solution NMR (Fernández et al. 2001; Hagn et al. 2013). MD simulations have been carried out on OmpX either inserted in a lipid bilayer, or complexed by a detergent, or trapped in a phospholipid nanodisc (Böckmann and Caflisch 2005; Choutko et al. 2011; Hagn et al. 2013) and the organization of its complexes with A8-35 characterized in some detail by solution NMR (Catoire et al. 2009, 2010; Etzkorn et al. 2014). The stoichiometry of OmpX to A8-35 in the complexes, however, has not been experimentally determined. In the present work, a series of models were therefore first created, where the number of APol molecules randomly seeded in the simulation box at the onset of the calculation was progressively increased until their assembly saturated the protein's transmembrane surface. The structure and dynamics of the resulting complexes were then analyzed, with a focus on the interactions between MP and APol, the distribution of A8-35's various moieties in the APol belt, the shape of the belt, and the extent to which OmpX is shielded from water. In complexes with sufficient APol (here estimated to be up to 44 kDa of polymer per protein), the hydrophobic transmembrane surface of the protein is entirely shielded from water, whereas the APol forms minimal contacts with the protein's extramembrane surfaces, in excellent agreement with NMR data. A comparison of the dynamics of OmpX, either in complex with A8-35 or the detergent dihexanoylphosphatidylcholine (DHPC) or inserted into a dioleoylphosphatidylcholine (DOPC) bilayer, reveals that

the protein dynamics is restrained in APol, in possible support of the "Gulliver effect" hypothesis.

Methods

Simulations were performed using the Martini coarse-grained force field version 2.1 (Marrink et al. 2007). An elastic network model was used to stabilize the secondary and tertiary structure of OmpX, while obtaining realistic protein dynamics (Periole et al. 2009). For the initial OmpX structure, PDB ID 1qj8 was used (Vogt and Schulz 1999). We note that differences in loop lengths have been observed in recent NMR structures (Hagn et al. 2013). The setup of our simulations however precludes an investigation of environment-dependent changes in secondary structure. Parameters for amphipol A8-35 have been previously described (Perlmutter et al. 2011). Based on early experimental data, we used a polymer length of 45 units, though more recent measurements indicate that the average length of A8-35 is closer to $\sim$35 units (Giusti et al. 2014). This is without consequence, as previous work has shown that varying the length by twofold does not affect the results of the simulations (Perlmutter et al. 2011). To prevent variation due to grafting sequence, a single random sequence was used for all simulations, where U = ungrafted carboxylate, I = isopropyl grafted, O = octyl grafted:

OIIOUIUIOU UOOIIUUUII IIIUIUUUUU OIIOUOOUUI IOIOI.

For each system, our strategy consisted of two successive simulation steps: an assembly simulation, for which protein dynamics was strongly restrained, followed by a second, unrestrained simulation. In the initial assembly simulations, each CG unit of the protein was restrained using a positional restraint in each dimension with a potential of 1 kJ mol^{-1} nm^{-2}, intended to drastically limit protein dynamics and prevent unfolding of the protein before assembly occurs. In the second step, these restraints are removed. However we do make use of an elastic network model which has been shown to retain realistic protein dynamics (Periole et al. 2009). In the assembly simulations, the protein and either an adjustable number of A8-35 molecules or 125 DHPC molecules were initially placed separately in the simulation box. This number of DHPC molecules results in the formation of an oblate detergent belt around OmpX (Böckmann and Caflisch 2005). The simulations contained 32,000–35,000 water molecules and neutralizing counterions. This corresponds to $\sim$0.5 mM OmpX, and either $\sim$1.6–4.9 mM APol or 50 mM DHPC. Assembly simulations were run for 10 μs each, and each system was run in triplicate, varying the initial velocities. In each case, an assembled complex is formed in this time period, with no APol molecules remaining unassembled. For the lipid bilayer simulations, the protein was similarly restrained during an initial 10 μs period, but, in the initial configuration, it was inserted in a bilayer comprised 258 DOPC molecules, at full hydration (43.4 waters/lipid). For each system, following 10 μs of restrained dynamics, subsequent unrestrained simulations were also run for 10 μs, in order to describe protein dynamics within the complexes.

All simulations were performed using Gromacs version 4.5 (Hess et al. 2008). The isotropic simulations were run in the NPT ensemble, using a pressure of 1 atm and a temperature of 303 K. Pressure was controlled using the Berendsen isotropic pressure coupling scheme. Bilayer simulations were run using a semiisotropic pressure coupling scheme. Simulations were run with a timestep of 30 fs. Analysis was performed using Gromacs and visualization with VMD (Humphrey et al. 1996).

Results

Formation of OmpX/A8-35 Complexes and Shielding of the Protein from Water

In order to build models of OmpX/A8-35 complexes, a series of coarse-grained simulations were run at varying OmpX/A8-35 ratios. To obtain an equilibrium structure unbiased by a designed starting configuration, these simulations were begun with the components diffuse in the simulation box. During the initial 10 μs of simulation, the protein was restrained to prevent unfolding. Over this period, the APol strands wrapped around the protein, forming a stable complex. These simulations were run in triplicate, and their agreement suggests that equilibration was obtained, as will be shown in the analysis below. The results presented in this section come from these restrained simulations. Following this assembly step, one simulation of each setup was extended in the absence of the positional restraints for a further period of 10 μs in order to explore the structure of the complex and the protein dynamics (described below). An identical protocol was used to simulate OmpX/DHPC complexes, in order to compare the effects of the APol with those of a detergent. The simulation strategy for OmpX in a DOPC bilayer was similar, except that the starting configuration was obtained by inserting OmpX into a preformed DOPC bilayer.

Figure 1 shows snapshots from the end of the assembly simulations. The surface interacting with the hydrophobic domain of the protein appears to be largely composed of hydrophobic, octyl chains, and the outer surface is richer in ungrafted carboxylates. For systems containing 4 or 6 A8-35 chains (22 and 33 kDa, respectively), there appears to be

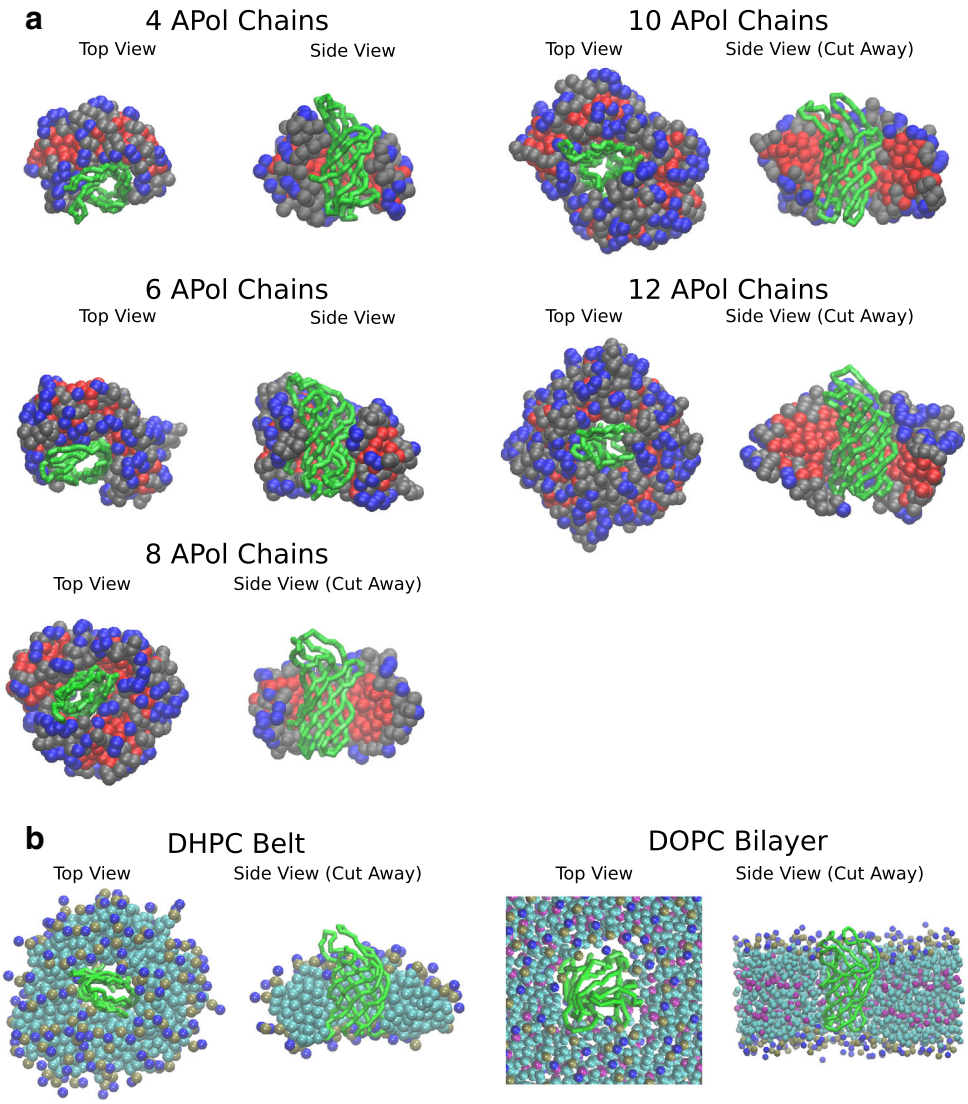

Fig. 1 Snapshots illustrating the configuration of **a** OmpX/A8-35 and **b** OmpX/DHPC and OmpX/DOPC complexes after 10 μs of dynamics. For each system, the *left column* shows the top view (corresponding to the extracellular surface of the protein), the *right column* a side view or side view with cutaway. Color scheme: *green* OmpX, *red* octyl chains of APol, *gray* isopropyl chains of APol, *blue* carboxylates of APol, *blue* choline moiety of DHPC/DOPC, *tan* phosphate moiety of DHPC/DOPC, *cyan* methylene groups of DHPC/DOPC, *purple* methine groups of DOPC (Color figure online)

insufficient polymer to completely envelop the central, hydrophobic domain of the protein. For systems containing 8, 10, or 12 chains (44, 55, and 66 kDa, respectively), the polymers fully wrap 360° around the protein. Interestingly, even as further APol is added to the system, the extramembrane loops of the protein remain free, interacting with the solvent and, occasionally, with ungrafted carboxylates, rather than with octyl chains. The binding of DHPC and DOPC to the protein seems to follow a similar pattern (see below).

In Fig. 2, the relative extent to which each residue of the protein is shielded from solvent by the APol is plotted along the sequence for three independent simulations. It is compared to the NMR observations of Catoire et al. (2010) where hydrogen/deuterium exchange was used to determine the solvent accessibility of peptide groups in OmpX/A8-35 complexes. The experimental data are quantified through a relative protection factor, where the residue least exposed to water is given a value of 1, and all other residues are normalized relative to this amino acid (Catoire et al. 2010). Simulation data were analyzed following a similar protocol: first calculating the number of waters interacting with (i.e., within 1 nm from) the backbone of each amino acid, and then normalizing to the most protected residue. The H/D exchange rate could be influenced by other factors besides solvent accessibility which are not included in the simulation analysis, such as local pH effects due to electrostatic interaction between charged sidechains and ungrafted carboxylates (Kim and Baldwin 1982). Comparison of the distribution of NMR protection data and MD water contacts in Fig. 2 suggests that a single basic residue (Arg72) could be affected by such an effect. This residue, although positively charged, is also poorly accessible to a negatively charged quenching agent (Etzkorn et al. 2014) (see below).

The first observation is that for each system, the three independent simulations result in very similar profiles,

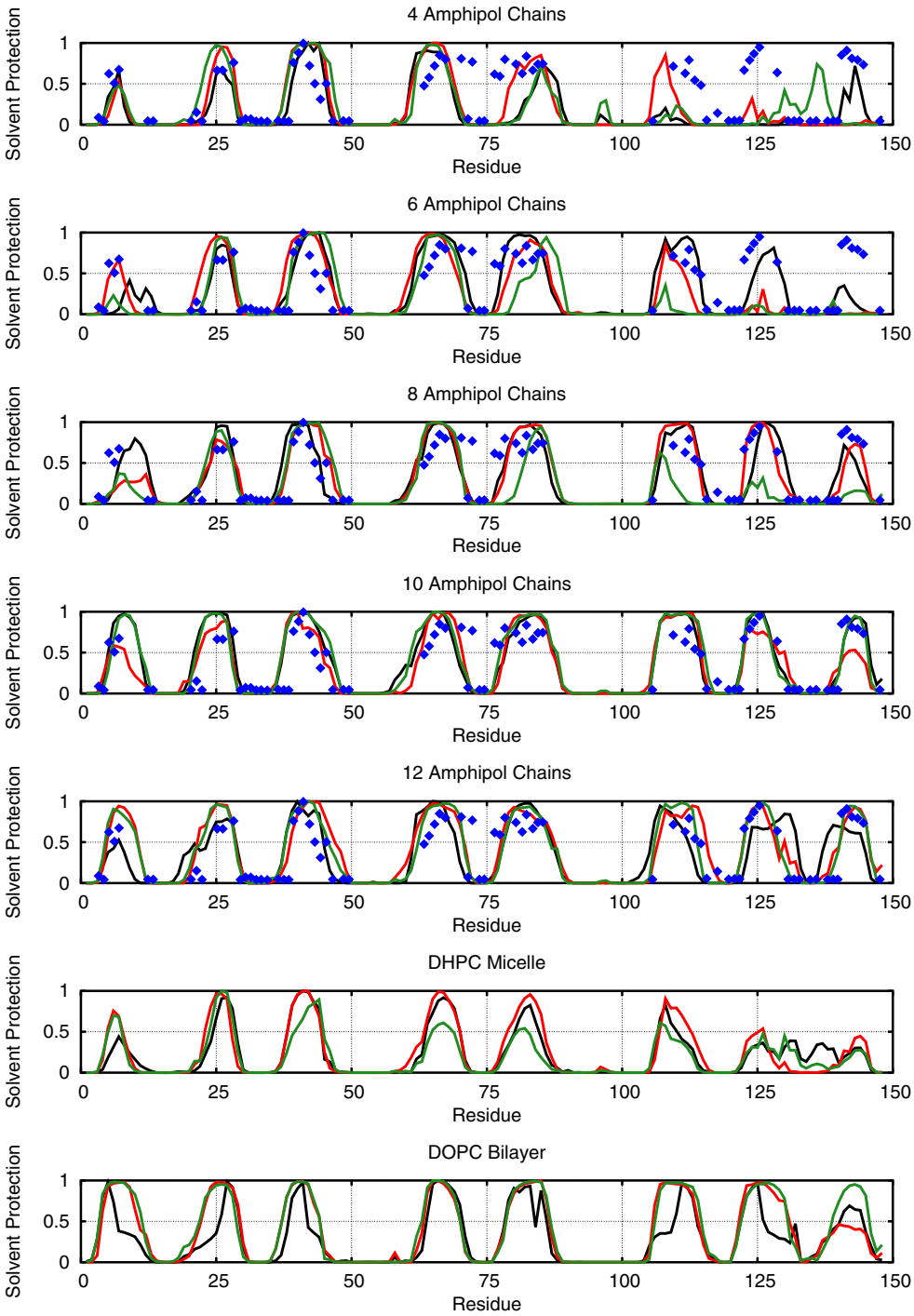

Fig. 2 Relative solvent protection of the backbone of OmpX in different environments. *Each line* represents an independent simulation. Experimental accessibility of peptide bonds in OmpX/A8-35 complexes, based on the rate of H/D exchange (Catoire et al. 2010), is shown as *blue diamonds* (Color figure online)

suggesting that the timescale of the simulation is appropriate for equilibration. Broadly, the results of the simulations and experiment are similar, with the β-strands shielded and the hydrophilic loops exposed. Free exposure of the loops and turns to the solvent is consistent both with H/D exchange data (Catoire et al. 2010) and with the degree of accessibility of amide protons to a water-soluble paramagnetic agent (Etzkorn et al. 2014).

Interestingly, the simulations that use what appears to be insufficient APol (4 and 6 chains) show that the polymer seems to preferential shield strands 2–5 (numbered starting from the *N*-terminus), and consistently leaves the most *N*-terminal and three *C*-terminal strands exposed. Analysis using the Kyte–Doolittle hydrophobicity scale with a sliding window suggests that the second, third, and fourth strand are the most hydrophobic (Kyte and Doolittle 1982).

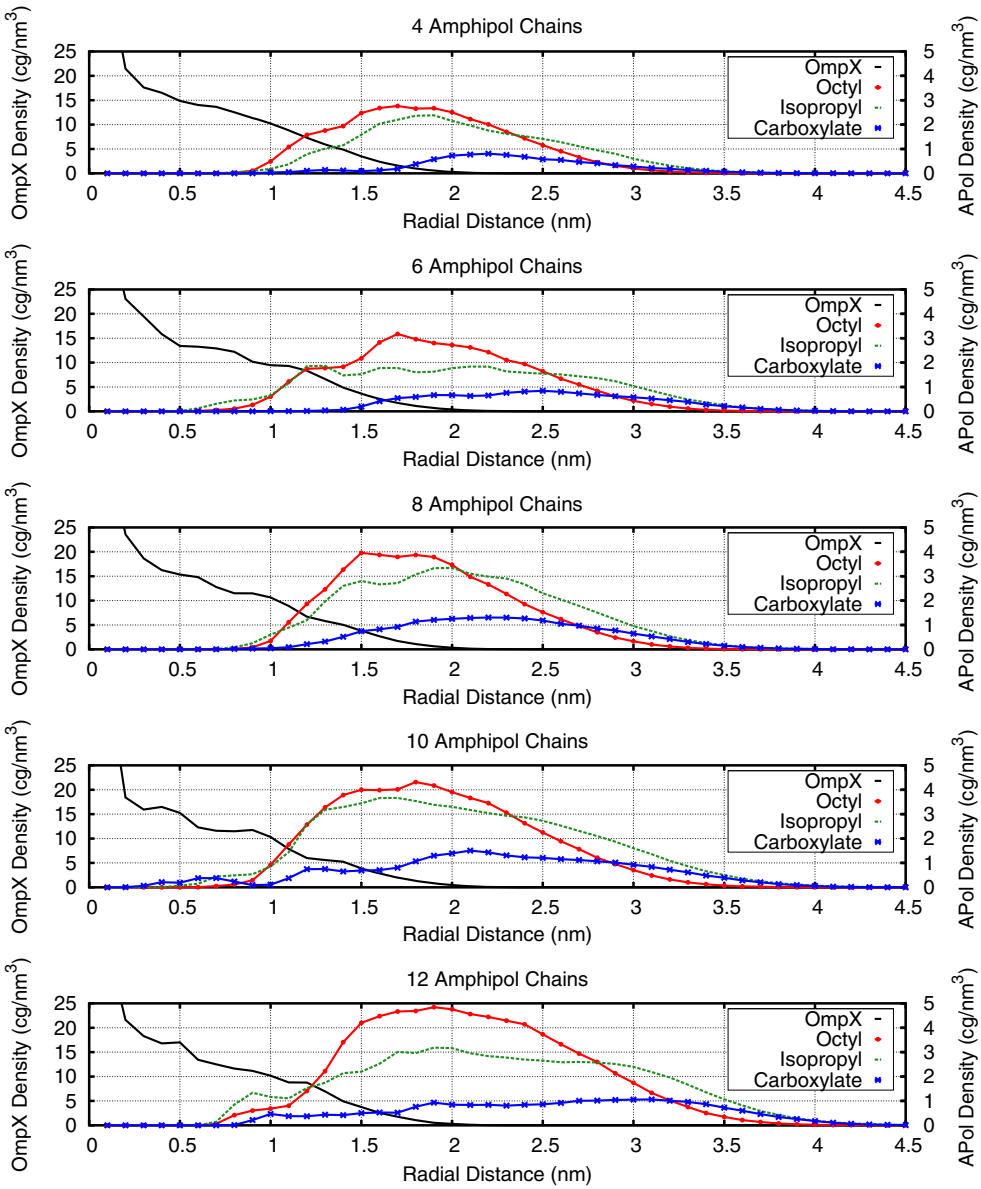

Fig. 3 Radial density of various moieties in OmpX/A8-35 complexes calculated by aligning the axis of the β-barrel with the *z*-axis, and recording the radial density of components in a 2-nm-thick cylindrical slab surrounding the central region of the barrel

For the system with 8 chains, all β-strands are shielded, presenting a qualitative match to the experimental data. By reference to experimental estimates of A8-35 binding by the transmembrane domain of OmpA, a similar 8-strand β-barrel (∼25 kDa, but likely to be an estimate by default) (Zoonens et al. 2007), and BR, a larger, 7-α-helix MP with bound lipids (∼54 kDa) (Gohon et al. 2008), one can surmise that 44 kDa is more likely to be an over- than an underestimate of the amount of A8-35 that binds to OmpX in actual experiments. Further additions of APol (up to 10 and 12 chains) do not increase the shielding of the loops and turns, which remain exposed in all cases. There is a small change in the most *N*-terminal strand, which is less shielded than the other strands in the complexes with 4, 6, and 8 chains, in agreement with the experimental data, but whose shielding increases in the systems with 10 and 12 chains. On this basis, the simulated 8-chain system appears closest to the experimental one. The continuous accretion of further APol molecules above this ratio may well be an artifact of the simulation conditions, under which the APol is much more concentrated than it is in real circumstances. Interestingly, for the system with DHPC, the two *C*-terminal strands are less efficiently shielded than in APol, whereas in the DOPC bilayer, the shielding profile looks similar to that of APol with ≥8 chains.

A comparison of our model with recent experimental measurements of OmpX accessibility to a water-soluble paramagnetic agent similarly yields strong agreement

(Etzkorn et al. 2014). In this recent work, the authors identified 15 residues which were solvent-exposed and 56 which were shielded. If we define a residue to be solvent-exposed if it is in contact with water for >95 % of the simulation duration, we find best agreement with these data for our system containing 8 chains. In this case, our simulation agrees with the experiment for 65 of 71 residues. The discrepancies are in the terminal residues of the β-strands on the intracellular side, which are only moderately shielded in our simulations. As noted above, Arg72 appears more shielded from both H/D exchange and quenching in NMR experiments than from water in MD simulations, possibly due to its interactions with A8-35 carboxylates.

The Amphipol Belt

The structure of the hydrophobic region of the complex is described in Fig. 3 by the radial distribution of its components, averaged over the three models generated for each OmpX/APol ratio. In this analysis, the central axis of the β-barrel is aligned with the *z*-axis, and the radially averaged local density of the protein and APol moieties is plotted against the distance from this axis in the plane defined by the *x*- and *y*-axes. To focus on the hydrophobic region, the analysis is limited to a 2-nm slab around the mid-plane of the membrane, defined by the mid-point of the barrel. Whatever the amount of bound APol, one observes a higher density of the octyl and isopropyl side chains of the polymer close to the surface of the protein, whereas the free carboxylates lie at larger radial distances. Note that this non-random distribution occurs despite the random sequence of the polymer.

The radially averaged density around the central domain of the protein is informative, but, in order to emphasize the lack of radial symmetry around the protein, Fig. 4 presents two-dimensional (2D) density distributions of the polymer looking down the *z*-axis, which has been aligned with that of the barrel and is placed at the origin. The protein is oriented in the same manner in all three panels. The same equilibrium distributions are obtained for the three models built at each protein/APol ratio (not shown), confirming that they are genuine equilibrium distributions and are not due to random fluctuations.

As suggested by the snapshots in Fig. 1, the time-averaged thickness of the APol coat around the protein is non-uniform. In the system with an insufficient amount of APol (6 chains), the more hydrophobic strands (2–5) are shielded whereas the *C*-terminal strands are not (upper left vs. lower right quadrants). Even in the first model with enough APol (8 chains) to fully cover the transmembrane region of the protein, the thickness of the APol layer appears to be greater around strands 2–5 as compared to the *N*-terminal and *C*-terminal strands. In the model with excess A8-35, the thickness of the APol belt increases, but still certain regions of the protein have thicker belts than others. Interestingly, the APol bulge in the lower-left quadrant of the 8- and 10-chain models appears to consist of many self-associated octyl chains, only some of which directly interact with the protein surface, while others are more distant (>1 nm). On the one hand, this could be taken as an indication that the 8-chain models have perhaps more APol bound than actual OmpX/A8-35 complexes. On the other, this non-uniformity of the APol belt around the surface of the protein is reminiscent of the "bumpiness" experimentally observed in EM reconstructions of an A8-35-trapped mitochondrial supercomplex, which also was reproducible from one set of data to the other (Althoff et al. 2011). As discussed below, a better understanding of this phenomenon could possibly provide insights into improving the chemistry and physical properties of APols.

In order to describe the OmpX/APol complex structure in both the hydrophobic and hydrophilic regions of the protein, we calculated the most frequent interaction partner for each OmpX residue, for the system containing 8 APol chains (Fig. 5). As has already been described above, the β-strands interact primarily with the octyl and isopropyl grafts of the polymer and have much less interaction with water or the ungrafted carboxylate segments. Panel B clarifies the interactions in the loop and turn regions of the protein. In most cases, the interaction with water is more frequent than that with the free carboxylates of the polymer. However, there are several regions where this interaction is frequent and these peaks coincide with positively charged amino acids residues. In all cases where interaction with carboxylates occurs during more than half of the simulation time, there is a positive charged side-chain, specifically Lys20, Arg72, Lys89, Arg131, Arg133, and Arg147, and other, smaller peaks also coincide with the locations of arginines or lysines. The propensity of A8-35 to form such electrostatic contacts may affect its interactions with highly basic proteins (cf. Champeil et al. 2000). These data are illustrated in Fig. 6 by differential coloring of the 3D structure according to the most prevalent interaction partner of each amino acid residue.

Experimental data on the organization of protein–APol complexes have been previously reported and present an opportunity for comparison. The thickness of the APol belt in our models has been quantified by the full width at half-maximum (FWHM) of the radial density. For the complex with 8 chains, which is the smallest amount of APol for which the transmembrane region of the protein is totally surrounded and which qualitatively matches the NMR protection data (Catoire et al. 2010; Etzkorn et al. 2014), the belt FWHM thus estimated is $\sim$1.57 nm. This is consistent with experimental observations, which suggest belt thicknesses of 1.5–2 nm for complexes between A8-35

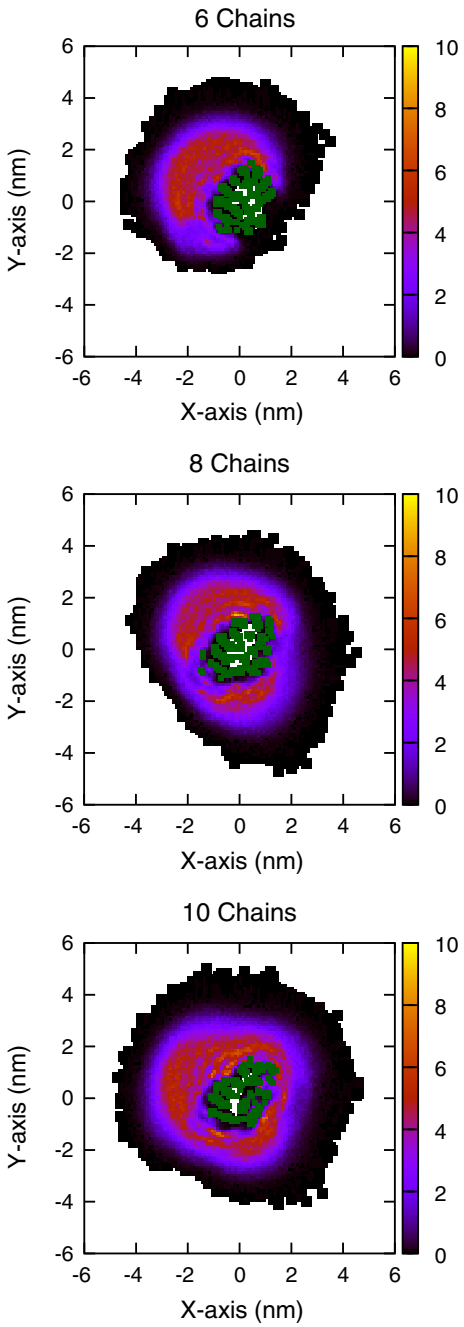

Fig. 4 Time-averaged two-dimensional APol densities in a 2-nm-thick cylindrical slab surrounding the central region of the β-barrel, showing that the polymer density is not radially symmetric. *Green* indicates regions of significant protein density (>7.5 CG segments nm^{-2}) (Color figure online)

and either BR (Gohon et al. 2008) or a mitochondrial supercomplex (Althoff et al. 2011). In Fig. 7, the radius of gyration of the particles is plotted as a function of the OmpX/A8-35 ratio. Notably, independent simulations result in nearly identical radii (the error bars describing the standard error associated to R_g when treating the separate simulations as independent samples are smaller than the data points). As expected, the radius increases with the number of APol chains, but it remains less than that of the oblate OmpX/DHPC complexes. Experimentally, OmpX/DHPC complexes appear to tumble more rapidly than OmpX/A8-35 ones (Fernández et al. 2001; Catoire et al. 2010), suggesting that the MD model may have too much DHPC bound.

Dynamics of A8-35-Trapped Versus Detergent-Solubilized and Membrane-Bound OmpX

The dynamics of a protein is often closely linked to its activity. As mentioned in the introduction, it has been speculated that some of the functional effects of APols, as well as part of their stabilizing character, may be a consequence of their ability to damp the dynamics of MP transmembrane domains (Popot et al. 2003, 2011; Picard et al. 2006). In the simulations presented in the above sections, the complexes were equilibrated with the protein dynamics restrained, in order to prevent unfolding. In the following simulations, this strong positional restraint has been removed in order to describe the protein dynamics within the equilibrated complex.

Figure 8 shows the protein root mean squared fluctuations (RMSF), which describe the conformational flexibility of its backbone at each amino acid. The general profile shows lower values (restrained dynamics) for the β-strands and larger values (increased flexibility) for the loops and turns. As more APol is added to the system, the protein dynamics becomes increasingly restrained, until 8 chains have been added (Fig. 8a), at which point additional APol has no observable effect (*not shown*). Interestingly, whereas the models with 4 and 6 chains seem to effectively shield the *N*-terminal strands while leaving the *C*-terminal ones exposed (Fig. 2), the difference with the 8-chain model is global: the protein dynamics is reduced at all positions upon moving from 33 to 44 kDa of bound APol and, thereby, completing the APol belt. Based on the structural observations described above, 8 chains seem to provide an appropriate model for the OmpX/A8-35 complex. Comparison of the protein dynamics in the presence of either A8-35, DHPC, or DOPC shows reduced conformational flexibility in the presence of the APol (Fig. 8b). Whereas the dynamics of the barrel are very generally damped in A8-35, there is a differential effect on the loops, the dynamics of the relatively long extracellular loops being more strongly affected than that of the short periplasmic turns. Also worth noting are subtle differences between OmpX solubilized in DHPC and inserted into the lipid bilayer, as has been recently described (Choutko et al. 2011).

Because trapping with APols affects the functionality of SERCA1a, whose transmembrane domain undergoes large-

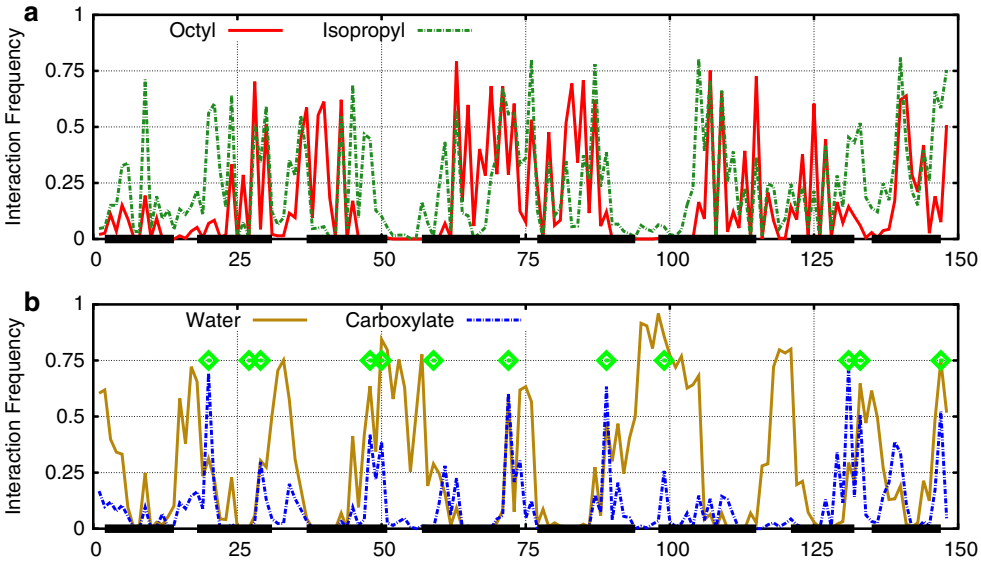

Fig. 5 Frequency with which each amino acid interacts with various polymer moieties or with water, for OmpX with 8 APol chains. For clarity, **a** presents hydrophobic components and **b** hydrophilic ones. *Thick black lines* indicate the location of β-strands, *green diamonds* that of basic amino acids (Lys and Arg)

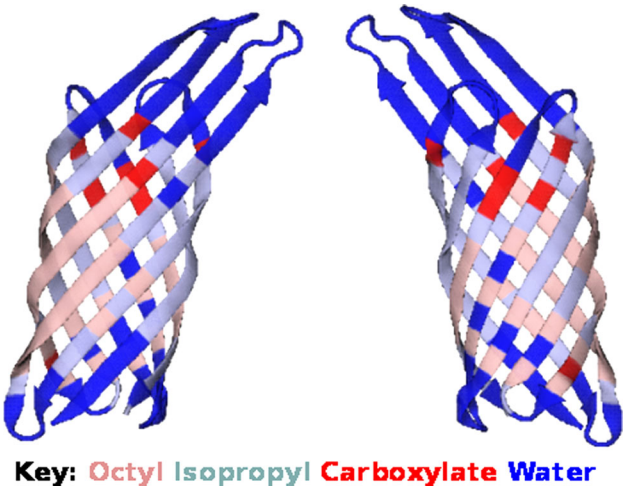

Fig. 6 Each amino acid in the 3D structure of OmpX (PDB ID 1qj8) is colored according to the nature of the partner it most frequently interacts with during the 8-chain simulation, using data from Fig. 5. *Left N*-terminal strands, *right C*-terminal strands. Color scheme: *pink* octyl chains of APol, *light blue* isopropyl chains, *red* carboxylates, *dark blue* water (Color figure online)

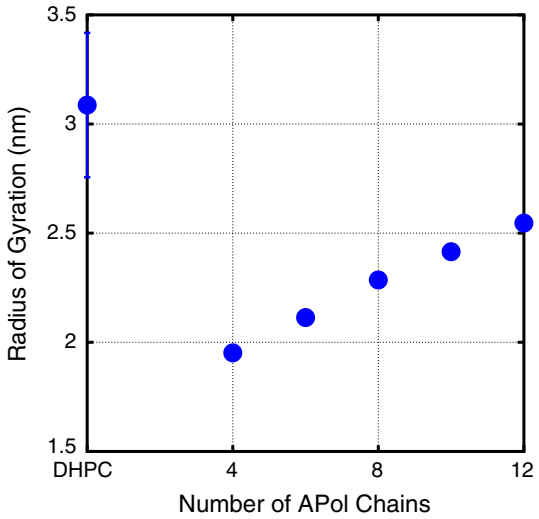

Fig. 7 Radius of gyration of the OmpX/DHPC and OmpX/A8-35 complexes, showing the effect of increasing the APol:OmpX ratio

scale (nanometric) conformational transitions during its enzymatic cycle (Champeil et al. 2000; Picard et al. 2006), but not, or much less, those of BR (Gohon et al. 2008; Dahmane et al. 2013) or the nicotinic acetylcholine receptor (Martinez et al. 2002), whose transmembrane conformational changes are more subtle, it has been speculated that large movements are more severely damped than small ones (Popot et al. 2003, 2011; Picard et al. 2006). Principal component analysis (PCA) was used to describe dynamics independently at longer and shorter length scales. In Fig. 9a, the principal components of the protein dynamics are presented for OmpX in A8-35, DHPC, and DOPC. Each eigenvector describes a single degree of collective motion, with lower indices corresponding to larger length-scale motions. The corresponding eigenvalues describe the magnitude of fluctuations along that degree of motion—essentially a mean squared fluctuation for each eigenvector. The results of this analysis are consistent with those of Fig. 8: the protein dynamics is more restrained in the complex with sufficient APol (8 or more chains) compared with the system with less APol (4 chains; *not shown*), and it is more restrained in the complex with 8 APol chains than it is in DHPC or DOPC (Fig. 9a). This analysis enhances our description of dynamics by clarifying that modes of motion on all accessible length-scales are restrained: the eigenvalues for the protein in the

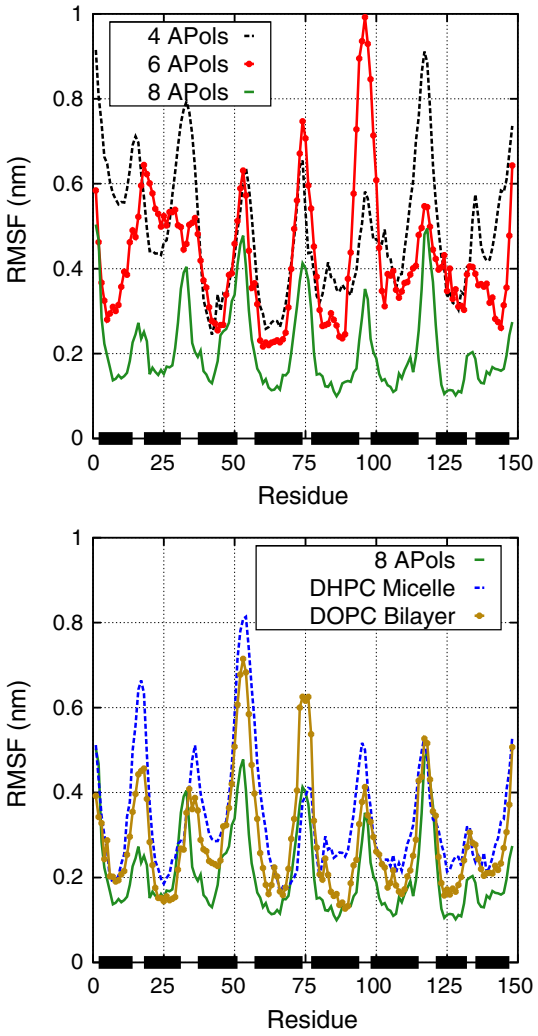

Fig. 8 RMSF of the protein backbone in complexes simulated without restraint

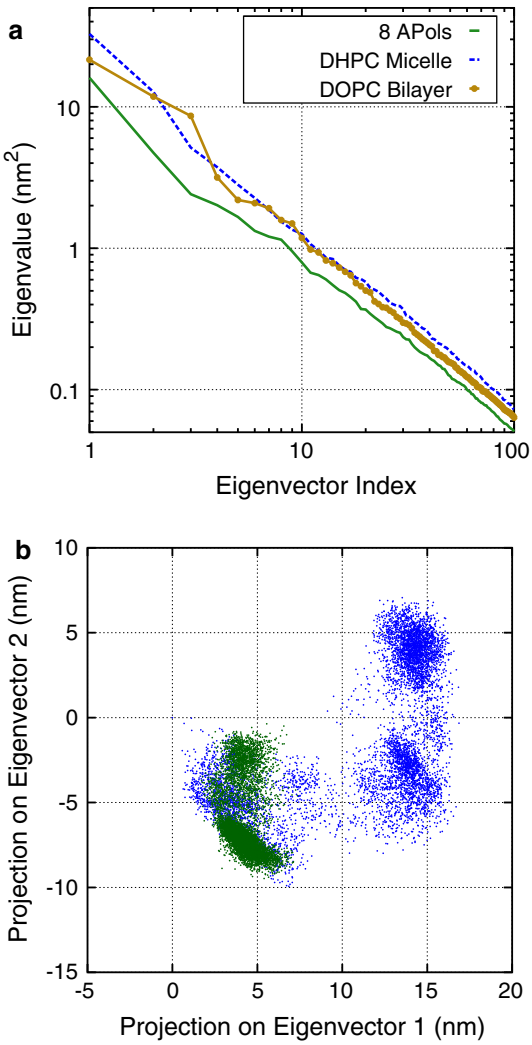

Fig. 9 **a** Eigenvalues for principal components of the protein dynamics in different environments. **b** Projections onto the first and second principal components for OmpX in the 8-APol chain and DHPC models

8-chain complex are lower than in DHPC or DOPC for all of the first 100 eigenvectors.

Figure 9b describes the restriction of the largest length-scale dynamics of OmpX in A8-35 versus DHPC. Each blue point corresponds to one frame from the simulation of OmpX in DHPC projected onto a 2D grid, where the *x*-axis indicates the displacement along the lowest-index principal component and the *y*-axis indicates displacement along the second lowest-index principal component. The first component appears as a twisting of the barrel and the second component as a radial widening and compressing degree of motion. In green, the frames from the simulation containing 8 APol chains are projected onto the same axes. Whereas there are substantial structural fluctuations for the protein in DHPC, these dynamics are largely restrained in APol.

To understand the relationship between the dynamics of the protein and its environment, we calculated the duration for which the hydrophobic groups of the APol (octyl chains), DHPC (hexanoyl chains), and DOPC (oleoyl chains) are in contact with the hydrophobic domain of the protein. These residence times were fit to an exponential decay, revealing very similar decay constants for A8-35 and DHPC (0.87 and 1.06 ns, respectively), and a somewhat longer one for DOPC (2.16 ns). It does not seem, therefore, that the damped dynamics of OmpX in A8-35 versus DHPC is the result of a restricted motility of the hydrophobic chains directly in contact with it.

Discussion

This study provides the first computational model of an APol-trapped MP. APols have proven very effective at

keeping MPs water-soluble while stabilizing them, thus allowing in vitro structural and functional studies under improved conditions, which can have a large impact in both basic and applied research. In order to fully exploit and improve this methodology, however, a great many issues remain to be clarified. Among those that can be explored using the present approach are the following: (i) What is the mode of association of the polymer with the protein? Does it affect its structure and/or dynamics? (ii) What are the mechanisms by which APols stabilize MPs? (iii) Which functional effects do they have?

As regards the organization of A8-35 around OmpX, MD data are remarkably consistent with existing experimental data: at saturation, the polymer forms a belt that covers exclusively and entirely the transmembrane, hydrophobic surface of the protein, as previously revealed by NMR and EM, and the thickness of the belt is similar to that observed experimentally. As expected, the octyl chains of A8-35 adsorb onto the hydrophobic surface of the protein, whereas free carboxylates lie farther from it and populate the surface of the belt. Contacts between the polymer and the extramembrane loops of OmpX are scarce and limited to the hydrophilic moieties of the polymer. An interesting observation is the reproducible formation, at a specific point of the barrel's surface, of a bulge of APol, reminiscent of those observed by EM at the surface of an A8-35-trapped mitochondrial supercomplex (Althoff et al. 2011). Because such bulges are not observed in the higher-resolution cryo-EM structure of another MP (Liao et al. 2013, 2014), it remains an open question whether they are real or may result from image reconstruction artifacts (for discussions, see Huynh et al. 2014; Zoonens and Popot 2014). It is difficult as well to determine if their presence in the MD models is a simulation artifact due to the very high concentration of APol present in the box and, possibly, an excess thereof as compared to equilibrium binding by OmpX. If the bulges are real, however, further analysis could provide clues toward identifying conditions—buffer composition or APol chemical structure—under which they do not form. This would make for smaller, more regular complexes, which could be of interest for certain applications, such as crystallography (cf. Charvolin et al. 2014).

As recalled above, a body of experimental observations suggests that trapping with APols may damp the dynamics of MPs, and that this may have the double effect of (i) stabilizing them, by creating a higher free-energy barrier to unfolding, and (ii) slowing down functional cycles that require large rearrangements of the protein/polymer interface. The present MD study brings some support to this hypothesis, inasmuch as it does show a damping effect of A8-35 as compared to DHPC, or even a DOPC bilayer. It also provides some further insights into this phenomenon. In its original form, the "Gulliver effect" hypothesis proposed that only relatively large-scale (nanometric) transmembrane movements were affected, which would account for the fact that, whereas most MPs are stabilized by transfer from detergent solutions to APols, only one of those hitherto studied, SERCA1a, sees its enzymatic cycle inhibited (Popot et al. 2003, 2011; Picard et al. 2006). It was speculated that protein conformational changes that could be accommodated by small movements of the octyl chains may not be strongly affected, whereas those requiring rearrangements of the polyacrylate backbone would. The present data lead to a more nuanced view, in the sense that (i) all movements appear to be damped, whatever their length scale, even though large-scale movements tend to be more strongly damped than small-scale ones; this may suggest that reasoning in terms of increased overall surface viscosity of the surfactant, as observed when comparing the polar surface of pure A8-35 particles with that of detergent micelles (Perlmutter et al. 2011), may be more appropriate than dissecting the molecular movements of the polymer; and (ii) the effect propagates to the extramembrane loops, even though those are not in contact with the polymer, or only minimally so. This opens the possibility that functional effects may be indirect. Clearly, the degree of functional perturbation possibly experienced by a number of MPs with different structures and functions will have to be studied in greater detail before a general picture can emerge. In the present simulations, we have only examined fluctuations of a small compact protein around a single equilibrium structure, and not large conformational changes in a complex multidomain protein such as SERCA1a. We also note that it is possible that certain types of motions may be less inhibited, for example a contractive motion, or conformational transitions in the extramembrane domains. It should also be kept in mind that there is now good evidence that some of the functional differences observed between detergent-solubilized and APol-trapped MPs may be due to lipid rebinding upon transfer to APols. This is clearly the case for the photocycle of BR (Dahmane et al. 2013), and it is suspected in that of the allosteric equilibria of the nicotinic acetylcholine receptor (Martinez et al. 2002). The methodology described here provides an interesting opportunity to explore the competition between APols, detergents, and lipids for binding sites at the surface of MPs.

In addition to examining more complex MPs and phenomena, MD can potentially help in the development of better APols. All APols used experimentally to date are polydisperse mixtures, and most of them feature a random distribution of hydrophilic and hydrophobic moieties along their chains. It is extremely time-consuming, and most often unrewarding, to explore systematically the effect of modifications to the chemical structure of APols, such as the length and length dispersity of the backbone, the nature of the hydrophilic and hydrophobic moieties, their

distribution, etc. In our previous simulations of A8-35 particles (without protein), we found that differences in grafting sequence could lead to changes in the size and shape of the polymer assemblies, whereas changing the backbone length did not (Perlmutter et al. 2011). It would be highly interesting, taking as a guide such criteria as the thickness and smoothness of the APol belt, or the dynamics of the protein, etc., to systematically explore by MD the effect of variations in chemical structure, so as to help the chemist and biochemist to develop better APols.

Acknowledgments Particular thanks are due to L. J. Catoire, M. Tehei, and G. Zaccai for discussions about the manuscript, as well as to a referee for useful comments. Computational resources were provided by the Minnesota Supercomputing Institute (MSI). This work was also supported by the French Centre National de la Recherche Scientifique.

References

Althoff T, Mills DJ, Popot J-L, Kühlbrandt W (2011) Arrangement of electron transport chain components in bovine mitochondrial supercomplex $I_1III_2IV_1$. EMBO J 30:4652–4664

Böckmann RA, Caflisch A (2005) Spontaneous formation of detergent micelles around the outer membrane protein OmpX. Biophys J 88:3191–3204

Catoire LJ, Zoonens M, van Heijenoort C et al (2009) Inter- and intramolecular contacts in a membrane protein/surfactant complex observed by heteronuclear dipole-to-dipole cross-relaxation. J Magn Reson 197:91–95

Catoire LJ, Zoonens M, van Heijenoort C et al (2010) Solution NMR mapping of water-accessible residues in the transmembrane beta-barrel of OmpX. Eur Biophys J 39:623–630

Champeil P, Menguy T, Tribet C et al (2000) Interaction of amphipols with sarcoplasmic reticulum Ca^{2+}-ATPase. J Biol Chem 275:18623–18637

Charvolin D, Picard M, Huang L-S, et al. (2014) Solution behavior and crystallization of cytochrome bc1 in the presence of amphipols. J Membrane Biol. doi:10.1007/s00232-014-9694-4

Choutko A, Glättli A, Fernández C et al (2011) Membrane protein dynamics in different environments: simulation study of the outer membrane protein X in a lipid bilayer and in a micelle. Eur Biophys J 40:39–58

Dahmane T, Rappaport F, Popot J-L (2013) Amphipol-assisted folding of bacteriorhodopsin in the presence or absence of lipids: functional consequences. Eur Biophys J 42:85–101

Etzkorn M, Zoonens M, Catoire LJ et al (2014) How amphipols embed membrane proteins: global solvent accessibility and interaction with a flexible protein terminus. J Membr Biol. doi:10.1007/s00232-014-9657-9

Fernández C, Adeishvili K, Wüthrich K (2001) Transverse relaxation-optimized NMR spectroscopy with the outer membrane protein OmpX in dihexanoyl phosphatidylcholine micelles. Proc Natl Acad Sci USA 98:2358–2363

Giusti F, Popot J-L, Tribet C (2012) Well-defined critical association concentration and rapid adsorption at the air/water interface of a short amphiphilic polymer, amphipol A8-35: a study by Förster resonance energy transfer and dynamic surface tension measurements. Langmuir 28:10372–10380

Giusti F, Rieger J, Catoire LJ et al (2014) Synthesis, characterization and applications of a perdeuterated amphipol. J Membr Biol. doi:10.1007/s00232-014-9656-x

Gohon Y, Pavlov G, Timmins P et al (2004) Partial specific volume and solvent interactions of amphipol A8-35. Anal Biochem 334:318–334

Gohon Y, Giusti F, Prata C et al (2006) Well-defined nanoparticles formed by hydrophobic assembly of a short and polydisperse random terpolymer, amphipol A8-35. Langmuir 22:1281–1290

Gohon Y, Dahmane T, Ruigrok RWH et al (2008) Bacteriorhodopsin/amphipol complexes: structural and functional properties. Biophys J 94:3523–3537

Hagn F, Etzkorn M, Raschle T, Wagner G (2013) Optimized phospholipid bilayer nanodiscs facilitate high-resolution structure determination of membrane proteins. J Am Chem Soc 135:1919–1925. doi:10.1021/ja310901f

Hess B, Kutzner C, van der Spoel D, Lindahl E (2008) GROMACS 4: algorithms for highly efficient, load-balanced, and scalable molecular simulation. J Chem Theory Comput 4:435–447

Humphrey W, Dalke A, Schulten K (1996) VMD: visual molecular dynamics. J Mol Graph 14:33–38

Huynh KW, Cohen MR, Moiseenkova-Bell VY (2014) Application of amphipols for structure-functional analysis of TRP channels. J Membr Biol. doi:10.1007/s00232-014-9684-6

Kim PS, Baldwin RL (1982) Influence of charge on the rate of amide proton exchange. Biochemistry (Mosc) 21:1–5. doi:10.1021/bi00530a001

Kyte J, Doolittle RF (1982) A simple method for displaying the hydropathic character of a protein. J Mol Biol 157:105–132

Liao M, Cao E, Julius D, Cheng Y (2013) Structure of the TRPV1 ion channel determined by electron cryo-microscopy. Nature 504:107–112

Liao M, Cao E, Julius D, Cheng Y (2014) Single particle electron cryo-microscopy of a mammalian ion channel. Curr Opin Struct Biol 27:1–7. doi:10.1016/j.sbi.2014.02.005

Marrink SJ, Risselada HJ, Yefimov S et al (2007) The MARTINI force field: coarse grained model for biomolecular simulations. J Phys Chem B 111:7812–7824

Martinez KL, Gohon Y, Corringer P-J et al (2002) Allosteric transitions of Torpedo acetylcholine receptor in lipids, detergent and amphipols: molecular interactions vs. physical constraints. FEBS Lett 528:251–256

Periole X, Cavalli M, Marrink S-J, Ceruso MA (2009) Combining an elastic network with a coarse-grained molecular force field: structure, dynamics, and intermolecular recognition. J Chem Theory Comput 5:2531–2543

Perlmutter JD, Drasler WJ II, Xie W et al (2011) All-atom and coarse-grained molecular dynamics simulations of a membrane protein stabilizing polymer. Langmuir 27:10523–10537

Picard M, Dahmane T, Garrigos M et al (2006) Protective and inhibitory effects of various types of amphipols on the Ca^{2+}-ATPase from sarcoplasmic reticulum: a comparative study. Biochemistry 45:1861–1869

Planchard N, Point É, Dahmane T et al (2014) The use of amphipols for solution NMR studies of membrane proteins: advantages and constraints as compared to other solubilizing media. J Membr Biol. doi:10.1007/s00232-014-9654-z

Pocanschi CL, Popot J-L, Kleinschmidt JH (2013) Folding and stability of outer membrane protein A (OmpA) from *Escherichia coli* in an amphipathic polymer, amphipol A8-35. Eur Biophys J 42:103–118

Popot J-L (2010) Amphipols, nanodiscs, and fluorinated surfactants: three nonconventional approaches to studying membrane proteins in aqueous solutions. Annu Rev Biochem 79:737–775

Popot J-L, Berry EA, Charvolin D et al (2003) Amphipols: polymeric surfactants for membrane biology research. Cell Mol Life Sci 60:1559–1574

Popot J-L, Althoff T, Bagnard D et al (2011) Amphipols from A to Z. Annu Rev Biophys 40:379–408

Swift J (1726) Travels into several remote nations of the world. In four parts. By Lemuel Gulliver, first a surgeon, and then a captain of several ships. Benjamin Motte, London

Tehei M, Giusti F, Zaccai G, Popot J-L (2014) Thermal fluctuations in amphipol A8-35 particles measured by neutron scattering. J Membr Biol (under review)

Tribet C, Audebert R, Popot JL (1996) Amphipols: polymers that keep membrane proteins soluble in aqueous solutions. Proc Natl Acad Sci USA 93:15047–15050

Vogt J, Schulz GE (1999) The structure of the outer membrane protein OmpX from *Escherichia coli* reveals possible mechanisms of virulence. Structure 7:1301–1309

Zoonens M, Popot J-L (2014) Amphipols for each season. J Membr Biol. doi:10.1007/s00232-014-9666-8

Zoonens M, Catoire LJ, Giusti F, Popot J-L (2005) NMR study of a membrane protein in detergent-free aqueous solution. Proc Natl Acad Sci USA 102:8893–8898

Zoonens M, Giusti F, Zito F, Popot J-L (2007) Dynamics of membrane protein/amphipol association studied by Förster resonance energy transfer: implications for in vitro studies of amphipol-stabilized membrane proteins. Biochemistry 46: 10392–10404